

Algorithmic Design and Resilience Assessment of Energy Efficient High-Rise Water Supply Systems

Lena C. Altherr¹, Philipp Leise¹, Marc E. Pfetsch²,
and Andreas Schmitt^{2*}

¹Chair of Fluid Systems, Technical University Darmstadt,
Otto-Berndt-Str. 2, 64287 Darmstadt, Germany

²Research Group Optimization, Department of Mathematics, Technical University Darmstadt,
Dolivostr. 15, 64293 Darmstadt, Germany
{altherr, leise, pfetsch, schmitt}@sfb805.tu-darmstadt.de

Keywords: MINLP, Resilience, Buffering Capacity, Uncertainty, Pump Systems, Booster Stations, Water Supply Networks

Abstract. High-rise water supply systems provide water flow and suitable pressure in all levels of tall buildings. To design such state-of-the-art systems, the consideration of energy efficiency and the anticipation of component failures are mandatory. In this paper, we use Mixed-Integer Nonlinear Programming to compute an optimal placement of pipes and pumps, as well as an optimal control strategy. Moreover, we consider the resilience of the system to pump failures. A *resilient system* is able to fulfill a predefined minimum functionality even though components fail or are restricted in their normal usage. We present models to measure and optimize the resilience. To demonstrate our approach, we design and analyze an optimal resilient decentralized water supply system inspired by a real-life hotel building.

Introduction

To supply the upper floors of tall buildings, pumps are mandatory. These pumps are usually placed at the lowest level. In [1] it was shown that a distributed placement of variable speed pumps has the potential of significant energy savings. To compute the optimal placement of the pumps together with the optimal connection of floors via pipes, a Mixed-Integer Nonlinear Program (MINLP) was presented. In fact, the optimization and design of water networks using MINLP techniques has been considered in several other publications, see, e.g., [2–5].

In this article, we consider the design of high-rise water supply networks such that disturbances in pump operation are tolerated. In particular, we consider the resilience of such systems, i.e., the system is able to fulfill predefined minimum requirements on the flow and pressure under uncertain failure situations. In the literature different approaches to and measures of resilience in water systems have been investigated, e.g., [6–8]. In this article, we consider resilience measured by the so-called *buffering capacity* of the system, i.e., the size of disruption that can be absorbed without fundamental breakdown in system performance [9]. This property holds in our context, if the system still fulfills the minimum requirements after the (complete) failure of K arbitrary pumps. In the traditional system layout, which places all pumps in the basement, this buffering capacity is achievable using redundant pumps. Our decentralized approach, however, has the potential to increase resilience through distributed placement of pumps and the possibility to employ more complicated pump network structures reducing the number of redundant pumps.

In the following, we introduce a mathematical optimization approach to design high-rise water supply networks that are resilient, measured using the buffering capacity. We first present a mathematical model of the initial system optimization without considering resilience. We then extend this model to compute optimal solutions with buffering capacity. To solve this model, we employ a branch-and-bound method. Finally, for an example building, we compute optimal solutions with buffering capacity K for $K = 1, 2, 3$ and evaluate their properties with respect to pump failures.

Mathematical Model

We first present a mathematical model that allows to compute an optimal placement of pipes and pumps as well as the optimal operation of pumps to supply a high-rise building with fresh water in a static case. It is a slightly modified version of the model given in [1]. The building is described by a graph $\mathcal{G} = (\mathcal{V}, \mathcal{A})$. The nodes $\mathcal{V} = \{0, \dots, N\}$ comprise the municipal water provider in node 0 and the $N \in \mathbb{N}$ pressure zones of the building. The arcs are given by $\mathcal{A} = \{(0, 1)\} \cup \{(u, v) \in (\mathcal{V} \setminus \{0\}) \times (\mathcal{V} \setminus \{0\}) : u < v\}$. Here, arc $(0, 1)$ represents the connection from the city water network to the building. The remaining arcs represent the possible pipes between the different pressure zones. We denote the sets of incoming and outgoing arcs of a node $v \in \mathcal{V}$ by $\delta^-(v) = \{(u, v) \in \mathcal{A} : u < v\}$ and $\delta^+(v) = \{(v, w) \in \mathcal{A} : w > v\}$, respectively. The design consists in deciding which potential connections, i.e., pipes, are built and where pumps are placed. In our model, built pipes are represented by binary variables x_a . We require that each pressure zone is connected to exactly one lower zone

$$\sum_{a \in \delta^-(v)} x_a = 1, \quad v \in \mathcal{V}. \quad (1)$$

The whole building has a water demand of D , which is evenly distributed to the pressure zones. Thus, the flow in each pipe q_a is determined by the pipe purchase decision and the flow equations

$$0 \leq q_a \leq D x_a, \quad a \in \mathcal{A}, \quad (2)$$

$$\sum_{a \in \delta^-(v)} q_a - \sum_{a \in \delta^+(v)} q_a = \frac{D}{N}, \quad v \in \mathcal{V}. \quad (3)$$

To compensate pressure loss due to friction and geodetic height differences, pumps can be build on bought pipes. We model a catalog of $C \in \mathbb{N}$ different pump types. On each bought arc up to $P \in \mathbb{N}$ pumps of the same type can be placed in parallel. Different types, on the other hand, are connected in series. Binary variables $y_{a,i}^p$ are used to model that on arc a type i was build p times in parallel. Naturally, we must decide the number of parallel pumps for each combination of pipe and type, yielding constraints

$$\sum_{j \in [P]} y_{a,i}^j \leq 1, \quad a \in \mathcal{A}, i \in [C], \quad (4)$$

where $[i] := \{1, \dots, i\}$ for a natural number i .

The model uses only variable speed pumps, which operate according to an empirical characteristic diagram provided by the pump manufacturer, compare Fig. 1. These diagrams describe the dependency of the potential pressure increase Δh and the power consumption p for a specific flow q and a normalized rotational speed ω . Different speed values are shown as contour lines in the figures. These contour lines are approximated by quadratic and cubic polynomials $f_i, g_i: \mathbb{R} \times \mathbb{R} \rightarrow \mathbb{R}$ for each pump type i following [10]. The approximations are

$$f_i(q, \omega) = \alpha_i^p q^3 + \beta_i^p q^2 \omega + \gamma_i^p q \omega^2 + \delta_i^p \omega^3, \quad \text{and}$$

$$g_i(q, \omega) = \alpha_i^h q^2 + \beta_i^h q \omega + \gamma_i^h \omega^2$$

for the power consumption and pressure increase, respectively, using coefficients $\alpha_i^p, \dots, \gamma_i^h$. In [11] it is shown, that parallel pumps of the same type are only controlled optimally if they run at the same speed, divide the flow of the zone uniformly and produce the same pressure increase. Thus, it suffices to include variables $\omega_{a,i}$, $\Delta h_{a,i}$ and $p_{a,i}$ to measure the relative running speed, the pressure increase and the power consumption of the pumps of type i on arc a , respectively. Further, the variables are connected by the constraints

$$p_{a,i} = \sum_{j \in [P]} j f_i \left(\frac{q_a}{j}, \omega_{a,i} \right) y_{a,i}^j, \quad a \in \mathcal{A}, i \in [C] \quad (5)$$

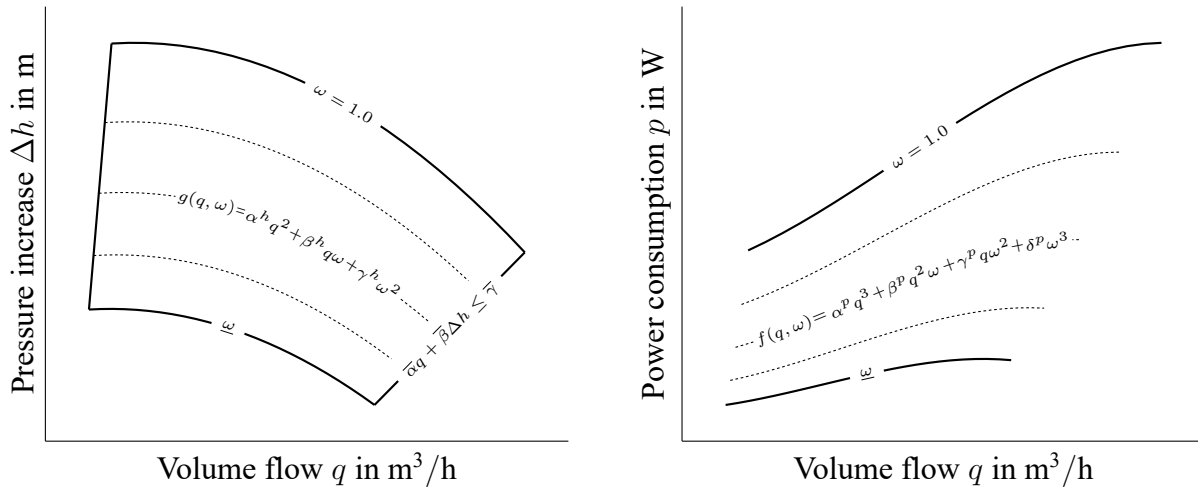


Fig. 1: Appearance of characteristic curves. Different values of ω appear as contour lines.

and

$$\Delta h_{a,i} = \sum_{j \in [P]} g_i \left(\frac{q_a}{j}, \omega_{a,i} \right) y_{a,i}^j, \quad a \in \mathcal{A}, i \in [C]. \tag{6}$$

The characteristic diagrams lead to more constraints. The scaled rotational speed of each pump type is bounded by $[\underline{\omega}_i, 1]$. In the $q-\Delta h$ diagram two more linear bounds on the feasible set can be seen. We include the right bound as a linear constraint

$$\left(\bar{\alpha}_i \frac{q_a}{j} + \bar{\beta}_i \Delta h_{a,i} - \bar{\gamma}_i \right) y_{a,i}^j \leq 0, \quad a \in \mathcal{A}, i \in [C], j \in [P]. \tag{7}$$

We neglect the left bound also appearing in the characteristic diagram. In our experience, it does not cut off optimal solutions, but increases the complexity of our resilience treatment.

The pressure in the building is measured in each pressure zone by variables h_v . They are lower bounded by a given minimal pressure H_{\min}

$$h_v \geq H_{\min}, \quad v \in \mathcal{V} \setminus \{0\}. \tag{8}$$

The pressure in node 0 is determined by the water supplier

$$h_0 = H_{\text{in}}. \tag{9}$$

In each zone v , the pressure is bounded by the pressure from the connected base zone u , the pressure increase of the pumps on the connecting arc and the pressure loss due to the change in geodetic height and due to pipe friction. We approximate the friction loss by a linear function of the pipe length. The pipe length is given by the height difference of two connected zones. Thus, the pressure loss can be combined with the height difference using a factor $R \in \mathbb{R}_+$, yielding the constraints

$$\left(h_v - h_u - \sum_{i \in [C]} \Delta h_{a,i} + R(v - u) \right) x_a = 0, \quad a = (u, v) \in \mathcal{A}. \tag{10}$$

We want to optimize investment costs as well as operating costs. The investment costs comprise pipe and pump investment costs, determined for each arc and pump type by C_a^{pi} and C_a^{pu} , respectively.

The operating costs include the power consumption of the pumps weighted by the constant C^{en} to include usage time and electricity rate. Combining all previous constraints yields the MINLP model

$$\begin{aligned}
\min \quad & \sum_{a \in \mathcal{A}} C_a^{\text{pi}} x_a + \sum_{a \in \mathcal{A}} \sum_{i \in [C]} \sum_{j \in [P]} C_i^{\text{pu}} j y_{a,i}^j + C^{\text{en}} \sum_{a \in \mathcal{A}} \sum_{i \in [C]} p_{a,i} \\
\text{s.t.} \quad & (1) - (10), \\
& x_a \in \{0, 1\}, q_a \in \mathbb{R}_+, & a \in \mathcal{A}, \\
& y_{a,i}^j \in \{0, 1\}, & a \in \mathcal{A}, i \in [C], j \in [P], \\
& \omega_{a,i} \in [\underline{\omega}_i, 1], \Delta h_{a,i}, p_{a,i} \in \mathbb{R}_+, & a \in \mathcal{A}, i \in [C], \\
& h_v \in \mathbb{R}_+, & v \in \mathcal{V}.
\end{aligned} \tag{11}$$

In practice, constraints (5), (6) and (7) are reformulated as big-M constraints, which is possible since the flow in the building and the speed of the pumps is bounded. The model given above uses some simplifications: Friction losses are approximated by a linear dependency on the pipe length. The quadratic dependency on the volume flow is not considered. Additionally, the solution is designed for the maximum volume flow demand of the building, which is only the case for a small proportion of the usage time.

Resilience

A system designed by solving Model (11) will provably be able to transport the given demand of water. However, no guarantees can be made if some of the built pumps are unavailable during operation due to failures or maintenance. To handle this uncertainty, we apply the concept of resilience. A *resilient technical system* guarantees a predetermined minimum of functional performance even in the event of disturbances or failures of system components. The functional performance of the high-rise water supply system is given by the maximal total flow demand the system can handle. To compare different solution designs according to their resilience, the following measure is introduced: The system has a *buffering capacity of K* , if every combination of up to K pump failures can be tolerated for a reduced volume flow demand D^{res} . In this context we also call it K -resilient. In the following sections we present models for resilience in detail. Moreover, we show a computationally feasible way to find a cost optimal system with a given buffering capacity. Finally, the impact of resilience is compared for different computed optimal solutions.

Model for resilience. In this section, we describe a model to check whether a system given by pipes x and pumps y has a buffering capacity of K for minimal demand D^{res} . Our main assumption is that energy costs are negligible during an emergency. Thus, after a failure, each remaining pump runs at maximal speed and Constraints (5), which determine the used power, can be ignored. We further assume that each group of parallel pumps also has a bypass installed, which is used when all pumps on a pipe have failed or are disabled. It is furthermore used to redirect the volume flow from the pumps, if it exceeds the pump's upper bound. This upper bound is implicitly given by the constraints of type (6) and (7).

To model resilience, the initial Model (11) is extended and analyzed. The subgraph induced by pipes x is an arborescence, i.e., a rooted directed tree, by Constraints (1). Thus, there exists for each pressure zone $v \in \mathcal{V}$ a unique 0 - v path denoted by $\mathcal{P}_x(v) \subset \mathcal{A}$. This has several implications. Using Constraints (2) and (3), the volume flows q^{res} and q for demands D^{res} and D , respectively, are determined by x . Also the pressure constraint (10) contain a telescoping sum and simplify together with (8) and (9) to

$$h_v = \sum_{a \in \mathcal{P}_x(v)} \sum_{i \in [C]} \Delta h_{a,i} + H_{\text{in}} - Rv \geq H_{\text{min}}, \quad v \in \mathcal{V} \setminus \{0\}.$$

Substituting $H_v := H_{\min} - H_{\text{in}} + Rv$ these inequalities further transform to

$$h_v = \sum_{a \in \mathcal{P}_x(v)} \sum_{i \in [C]} \Delta h_{a,i} \geq H_v, \quad v \in \mathcal{V} \setminus \{0\}.$$

For a fixed volume flow q in a pump, one can also determine the maximal pressure increase of a pump of type i built j times in parallel via the program

$$\begin{aligned} & \max \Delta h \\ & \text{s.t. } \Delta h \leq g_i\left(\frac{q}{j}, \omega\right), \\ & \quad \bar{\alpha} \frac{q}{j} + \bar{\beta} \Delta h \leq \bar{\gamma}, \\ & \quad \Delta h \in \mathbb{R}_+, \omega \in [\underline{\omega}, 1]. \end{aligned} \tag{12}$$

If this program is feasible, we denote its optimal objective value by $\overline{\Delta H}_i(q, j)$. Otherwise we set $\overline{\Delta H}_i(q, j) = 0$. We further introduce an encoding of possible pump malfunctions combinations in the set of failure scenarios

$$\mathcal{Z} := \{\tilde{z} \in \{0, \dots, P\}^{|\mathcal{A}| \times C} : \sum_{a \in \mathcal{A}} \sum_{i \in [C]} \tilde{z}_{a,i} \leq K\},$$

i.e., $\tilde{z}_{a,i}$ represents the number of type i pumps on arc a which are not operational. We bring y into the same dimension as \tilde{z} via the transformation

$$\tilde{y}_{a,i} := \sum_{j \in [P]} j y_{a,i}^j.$$

Combining the previous notation, the system (x, y) can withstand a failure scenario $\tilde{z} \in \mathcal{Z}$ with $\tilde{z} \leq \tilde{y}$ if and only if

$$\sum_{a \in \mathcal{P}_x(v)} \sum_{i \in [C]} \overline{\Delta H}_i(q_a^{\text{res}}, \tilde{y}_{a,i} - \tilde{z}_{a,i}) \geq H_v, \quad v \in \mathcal{V} \setminus \{0\}. \tag{13}$$

The design (x, y) has a buffering capacity of K if inequalities (13) hold for each $\tilde{z} \in \mathcal{Z}$. Since \mathcal{Z} grows exponentially in K , the verification of these inequalities is not computationally tractable in practice for larger K . Instead, we calculate for each pressure zone $w \in \mathcal{V} \setminus \{0\}$ the worst-case scenario \tilde{z} , which minimizes the pressure in zone w . This is done by solving the optimization problem

$$\begin{aligned} & \min \sum_{a \in \mathcal{P}_x(w)} \sum_{i \in [C]} \Delta h_{a,i} \\ & \text{s.t. } \Delta h_{a,i} \geq \overline{\Delta H}_i(q_a^{\text{res}}, j) (1 - z_{a,i}^j), \quad a \in \mathcal{P}_x(w), i \in [C], j \in [\tilde{y}_{a,i}], \\ & \quad \tilde{z}_{a,i} = \sum_{j \in [P]} z_{a,i}^j, \quad a \in \mathcal{P}_x(w), i \in [C], \\ & \quad \Delta h_{a,i} \in \mathbb{R}_+, \quad a \in \mathcal{P}_x(w), i \in [C], \\ & \quad z_{a,i}^j \in \{0, 1\}, \quad a \in \mathcal{P}_x(w), i \in [C], j \in [\tilde{y}_{a,i}], \\ & \quad \tilde{z} \in \mathcal{Z}. \end{aligned} \tag{14}$$

If for any zone w the optimal objective value is smaller than H_w , the design is not K -resilient. Problem (14) contains only linear inequalities since (x, y) is fixed. Its solving time scales well with K and N in practice. Thus, we described a feasible way to assess the resilience of a system and to compare different systems based on their buffering capacity. Note, that the model can also be used to identify weaknesses in the system, since a worst-case scenario is computed.

Optimal Design with Buffering Capacity K

In the following, we not only want to assess the buffering capacity of a system but also want to consider resilience in the design stage. Our goal is to find a system design with buffering capacity K for a demand D^{res} , which minimizes operating and investment costs, i.e., we want to solve Problem (11) under the added constraint (x, y) has buffering capacity K for D^{res} .

One way to handle this additional constraint in MINLP solvers is given by also including variables for the minimal volume flow q^{res} and pressure variables $h^{\tilde{z}}$ for each failure scenario $\tilde{z} \in \mathcal{Z}$ in Problem (11). To link the additional variables, inequalities resembling constraints of type (13) need to be included. This model would be very large due to the size of \mathcal{Z} . Moreover $\overline{\Delta H}_i(q_a^{\text{res}}, \tilde{y}_{a,i} - \tilde{z}_{a,i})$ would depend on q^{res} even though it is discontinuous in q^{res} . To treat this via MINLP techniques would require even more variables.

We therefore use a new way to find an optimal solution with buffering capacity K , presented in this section. The main idea is the following. As noted before, each solution topology represents a directed rooted tree in \mathcal{G} . Thus, it is possible to find an optimal solution by enumerating all trees and computing for each tree an optimal pump placement. An advantage of this enumeration is that the volume flow is fixed for a given tree. Thus, we can use $\overline{\Delta H}_i(\cdot, \cdot)$ without its discontinuous behavior in the computation of a K -resilient pump placement for the tree. We further deal with the large size of \mathcal{Z} by generating worst-case scenarios $\tilde{z} \in \mathcal{Z}$ dynamically. This is possible using the model of the previous section.

One disadvantage of the enumeration approach is the exponential growth of the number of trees in \mathcal{G} for increasing N . To balance this out, we use a relaxation, which has the potential to prune non optimal trees in the enumeration. We first present the computation of the pump placement for a fixed tree. Afterwards, the relaxation and the enumeration scheme are explained in more detail.

Optimal K -resilient design for fixed pipe topology. In this section, we consider a fixed pipe design x . For this topology, we present an algorithm to find an optimal pump purchase such that the whole system consisting of pipes and pumps has a buffering capacity of at least K . Recall, that the values of q^{res} and similarly the values of q are fixed by x . Additionally to $\mathcal{P}_x(v)$, we denote the used arcs of x by $\mathcal{A}_x := \{a \in \mathcal{A} : x_a = 1\}$. The following model computes the optimal pump purchase y for x which can withstand all failure scenarios of $\mathcal{Z}' \subseteq \mathcal{Z}$.

$$\begin{aligned}
\min \quad & \sum_{a \in \mathcal{A}_x} C_a^{\text{pi}} x_a + \sum_{a \in \mathcal{A}_x} \sum_{i \in [C]} \sum_{j \in [P]} C_i^{\text{pu}} j y_{a,i}^j + C^{\text{en}} \sum_{a \in \mathcal{A}_x} \sum_{i \in [C]} p_{a,i} \\
\text{s.t.} \quad & \sum_{j \in [P]} y_{a,i}^j \leq 1, & a \in \mathcal{A}_x, i \in [C], \\
& p_{a,i} = \sum_{j \in [P]} j f_i \left(\frac{q_a}{j}, \omega_{a,i} \right) y_{a,i}^j, & a \in \mathcal{A}_x, i \in [C], \\
& \Delta h_{a,i} = \sum_{j \in [P]} g_i \left(\frac{q_a}{j}, \omega_{a,i} \right) y_{a,i}^j, & a \in \mathcal{A}_x, i \in [C], \\
& \left(\bar{\alpha}_i \frac{q_a}{j} + \bar{\beta}_i \Delta h_{a,i} - \bar{\gamma}_i \right) y_{a,i}^j \leq 0, & a \in \mathcal{A}_x, i \in [C], j \in [P], \\
& \sum_{a \in \mathcal{P}_x(v)} \sum_{i \in [C]} \Delta h_{a,i} \geq H_v, & v \in \mathcal{V} \setminus \{0\}, \\
& \sum_{a \in \mathcal{P}_x(v)} \sum_{i \in [C]} \sum_{j \in [P]} \overline{\Delta H}_i(q_a^{\text{res}}, j - \tilde{z}_{a,i}) y_{a,i}^j \geq H_v, & v \in \mathcal{V} \setminus \{0\}, \tilde{z} \in \mathcal{Z}', \\
& y_{a,i}^j \in \{0, 1\}, & a \in \mathcal{A}_x, i \in [C], j \in [P], \\
& \omega_{a,i} \in [\underline{\omega}_i, 1], \Delta h_{a,i}, p_{a,i} \in \mathbb{R}_+, & a \in \mathcal{A}_x, i \in [C].
\end{aligned} \tag{15}$$

The first five constraint types are used to model the operation costs of the pump purchase and correspond to constraints of the initial model (11). The last constraint type ensures that the pressure in each zone is sufficient for the failure scenarios. In order to compute an optimal solution with buffering capacity of K it would suffice to solve the above model with $\mathcal{Z}' = \mathcal{Z}$. However, we use an iterative approach to keep the computational times low. Model (15) is solved for a subset \mathcal{Z}' of \mathcal{Z} , yielding a solution (x, y) . Using Model (14) for each pressure zone $w \in \mathcal{V}$, a worst-case scenario z is calculated for (x, y) . If these scenarios are not violated, the solution is resilient. Otherwise, we add the critical scenarios to \mathcal{Z}' and solve (15) again. This scheme will terminate, since \mathcal{Z} is finite. In practice, only a subset of scenarios is necessary, hopefully making this scheme faster than using the whole set.

Searching the pipe topology. We solve the problem of finding the optimal system with buffering capacity K by enumerating the finitely many possible pipe topologies and computing for each the optimal resilient pump purchase presented above. To avoid a complete enumeration, we present a model to compute lower objective bounds for the topologies. This relaxation is defined on a subtree $T = (\mathcal{V}_T, \mathcal{A}_T) \subset \mathcal{G}$ and is valid for all pipe topologies x with $\mathcal{A}_T \subseteq \mathcal{A}_x$. For some subtree, we calculate an estimation on the optimal pump placement with failure scenarios \mathcal{Z}' . We neglect all pressure zones not in \mathcal{V}_T yielding the volume flows $q_a, q_a^{\text{res}} \in \mathbb{R}_+$ determined by

$$\sum_{a \in \delta^-(v) \cap \mathcal{A}_T} q_a - \sum_{a \in \delta^+(v) \cap \mathcal{A}_T} q_a = \frac{D}{N}, \quad v \in \mathcal{V}_T \quad \text{and} \quad q_a^{\text{res}} = \frac{D^{\text{res}}}{D} q_a, \quad a \in \mathcal{A}_T.$$

Furthermore, only the zones in \mathcal{V}_T need to fulfill the minimal pressure bounds. The relaxation also uses the fact that f_i and g_i are assumed to be monotone in ω , i.e., an increase in operating speed increases the power consumption, but also yields a larger pressure increase for a pump. Thus, a lower bound on the power consumption is given by setting $\omega = \underline{\omega}$, whereas the pressure increase is upper bounded using $\overline{\Delta H}_i$. Since the relaxation considers the fixed subtree and the speed is estimated, the only free variables are the pump purchases y , yielding the problem

$$\begin{aligned} \min \quad & \sum_{a \in \mathcal{A}_T} C_a^{\text{pi}} + \sum_{a \in \mathcal{A}_T} \sum_{i \in [C]} \sum_{j \in [P]} j \left(C_i^{\text{pu}} + C^{\text{en}} f_i \left(\frac{q_a}{j}, \underline{\omega}_i \right) \right) y_{a,i}^j \\ \text{s.t.} \quad & \sum_{a \in \mathcal{P}_T(v)} \sum_{i \in [C]} \sum_{j \in [P]} \overline{\Delta H}_i(q_a, j) y_{a,i}^j \geq H_v, & v \in \mathcal{V}_T \setminus \{0\}, \\ & \sum_{a \in \mathcal{P}_T(v)} \sum_{i \in [C]} \sum_{j \in [P]} \overline{\Delta H}_i(q_a^{\text{res}}, j - \tilde{z}_{a,i}) y_{a,i}^j \geq H_v, & v \in \mathcal{V}_T \setminus \{0\}, \tilde{z} \in \mathcal{Z}', \\ & \sum_{j \in [P]} y_{a,i}^j \leq 1, & v \in \mathcal{V}_T, i \in [C], \\ & y_{a,i}^j \in \{0, 1\}, & a \in \mathcal{A}_T, i \in [C], j \in [P], \end{aligned} \tag{16}$$

where $\mathcal{P}_T(v)$ is the equivalent of $\mathcal{P}_x(v)$ for the tree T . Model (16) gives a lower bound of Problem (15) for fixed topology x , if $\mathcal{A}_T \subseteq \mathcal{A}_x$. To summarize, the relaxation is built by neglecting some pressure zones, using only a lower bound on the volume flow, using the maximal speed for the pressure increase but only the minimal speed for the power consumption of the pumps and including a subset of failure scenarios \mathcal{Z}' .

The enumeration of the possible pipe topologies is in depth-first order, beginning with the subtree $\mathcal{V}_T = \{0, 1\}$, $\mathcal{A}_T = \{(0, 1)\}$. A global set of failure scenarios \mathcal{Z}' is initialized to be empty. For each subtree, we calculate the relaxation value using (16). If the relaxation is infeasible or the value exceeds the value of a best found solution, the algorithm backtracks. Otherwise, the depth is increased by adding a new arc for the next subtree. If a subtree has maximal depth, i.e., $\mathcal{V}_T = \mathcal{V}$, optimal resilient pump purchases for the tree are generated. Model (15) is used to find solution candidates.

Table 1: Pump parameters.

Pump Type	Power				Pressure			$q\text{-}\Delta h$ bound (7)			ω	C^{pu}
	α^{p}	β^{p}	γ^{p}	δ^{p}	α^{h}	β^{h}	γ^{h}	$\bar{\alpha}$,	$\bar{\beta}$	$\bar{\gamma}$		
Type 1	-11.14	41.52	54.32	191.21	-3.42	2.76	45.19	60	-5	66	0.6	2344.55 €
Type 2	-1.77	5.90	135.81	245.28	-0.92	1.18	52.30	30	-5	68	0.6	2409.35 €
Type 3	-0.66	1.15	125.73	276.78	-0.35	0.37	47.97	14	-3	43	0.6	2484.75 €

Their buffering capacity is checked with Model (14). If the capacity is below K , a worst-case failure scenario is added to \mathcal{Z}' and a new candidate is computed. Otherwise, the optimal pump purchase is stored together with the pipe topology as a possible optimal solution of the whole scheme. Afterwards the algorithm backtracks. The solution with least costs is returned after the scheme enumerated the subtrees of \mathcal{G} . Note that, the set \mathcal{Z}' is only enlarged during the scheme.

Impact of Resilience Considerations

The solution scheme discussed in the previous section allows us to find optimal resilient systems for a moderate number of pressure zones. To investigate resilience, we compute the solutions of a real-world application for different resilience factors K .

Example building. We consider the Leonardo Royal Hotel building in Frankfurt am Main, Germany as an application example. This building has a height of 100 m and 451 rooms in total on 28 floors. We compute the volume flow and required pressure for the hotel based on the standard procedure in [12]. We assume that all floors have the same number of rooms and each room has the same sanitary components. Based on [12], we assume a volume flow of $1 \text{ m}^3/\text{h}$ and a total minimum pressure H_{\min} of 45 m in each floor. The pressure requirement is based on an assumed maximum pipe length in each floor. The pressure of the water supplier H_{in} is estimated with 45 m. We divide the building in $N = 7$ pressure zones. The pipe friction coefficient is estimated to be 0.05. Thus, the 100 m tall building with 7 pressure zones yields a value of 15 m for the parameter R used in Constraints (10). We prize the pipes with 5 € per meter. The costs for a pipe $a = (u, v)$ are therefore given by $C_a^{\text{pi}} \approx (v - u)71.43 \text{ €}$. For the energy costs we assume a price of 0.3 €/kWh and a operating time of 15 years with 350 days per year and 4 hours per day, so $C^{\text{en}} = 6.3 \text{ €/W}$. We allow $P = 5$ parallel pumps of the same model and use three different pump types with parameters shown in Table 1.

To solve the sub-problems in our solution scheme we used the framework SCIP 5.0.1 [13].

Results. Results. The optimal solution topologies with a buffering capacity of K for $K = 1, 2, 3$ and minimal volume flow $D^{\text{res}} = 0.8D$ are shown in Fig. 2. The figure also shows the normalized rotational speed of the pumps during regular operation. We observe, that the topologies of all solutions differ. Thus no solution is resilient for a K greater than the one it was designed for.

For $K = 0$, a multi-branched tree is built. After a failure of the pump on pipe (2, 4) the system is not able to transport the required flow to pressure zone 4.

The pipe topology changes drastically for the $K = 1$ solution. Here the tree has only two branches. The failure of two pumps on arc (0, 1) cannot be tolerated since a volume flow of $D^{\text{res}} = 22.4 \text{ m}^3/\text{h}$ must be processed by the remaining two pumps which can process around $8 \text{ m}^3/\text{h}$ each.

If two failing pumps are considered during optimization, the bought pipes form one single branch and another pump is added on arc (0, 1). However, again failures of pumps on this arc make the system fail, since the required demand cannot be provided.

The pipe topology for $K = 3$ is identically to the $K = 1$ case, but more pumps are placed on the basement arc (0, 1), while for $K = 1$ only pumps of Type 3 are placed. The $K = 3$ solution uses the pumps of $K = 1$ and additionally builds a pack of five parallel pumps of Type 2 in the basement. These pumps are only operated if another pump fails and are therefore redundant during regular operation. The additional pump type can be explained by the fact that only five parallel pumps of the same type are allowed on each arc.

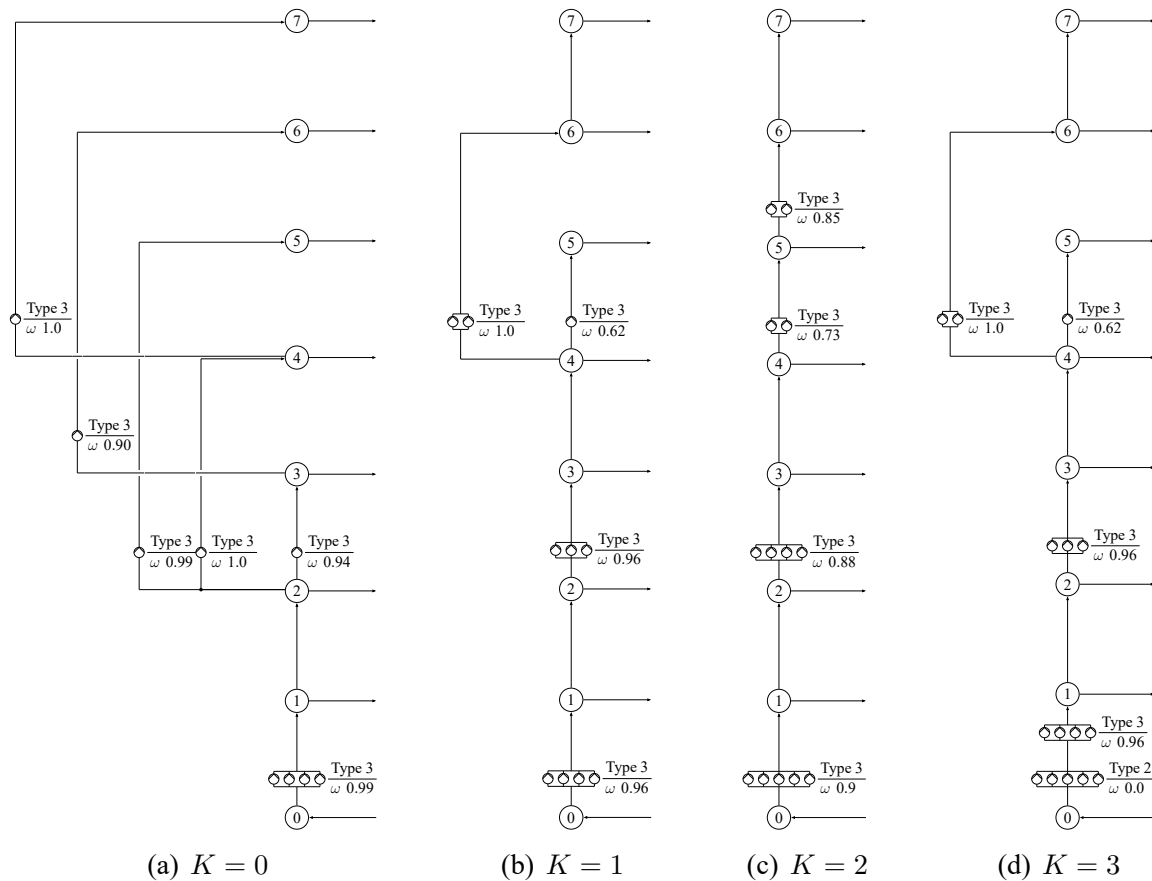


Fig. 2: Optimal solution topologies and the respective operating speeds ω for different buffering capacities K .

The operating and investment costs are presented in Table 2. The increased tolerance to pump failures results in higher overall costs, although these are mainly due to the higher number of built pumps. The system topology with a buffering capacity of zero is the most energy efficient one. This is illustrated by the nearly maximal operating speed of the placed pumps, whereas some pumps of the other solutions run under partial load.

We further notice that a simple strategy of redundancy to improve the $K = 0$ solution to be 1-resilient, which adds a pump for each built pack of pumps, would increase the investment costs by more than 50 %, whereas our computed resilient topology is only 8 % more expensive. Interestingly, the $K = 3$ optimal solution is only around 0.003 % cheaper than the optimal pump placement with buffering capacity of $K = 3$ computed for the one branch pipe topology seen in the $K = 2$ solution. It seems that for our parameters a good strategy to tolerate pump failures is given by reducing the number of branches in the tree. Furthermore, the solutions are highly dependent on the ratio of energy to investment costs.

Table 2: Investment and operating costs for varying buffering capacity.

Buffering capacity	0	1	2	3
Investment Costs	23, 291 €	25, 347 €	32, 730 €	37, 394 €
Operating Costs	48, 657 €	49, 692 €	48, 578 €	49, 692 €
Total Costs	71, 948 €	75, 039 €	81, 308 €	87, 086 €

The used operating points for the different topologies are shown in Fig. 3. Each point represents the rotational speed and volume flow of one pump of each used group. Our solution topologies consist of pumps of Type 2 and 3. However, during normal operation without failures, only pumps of Type 3 are

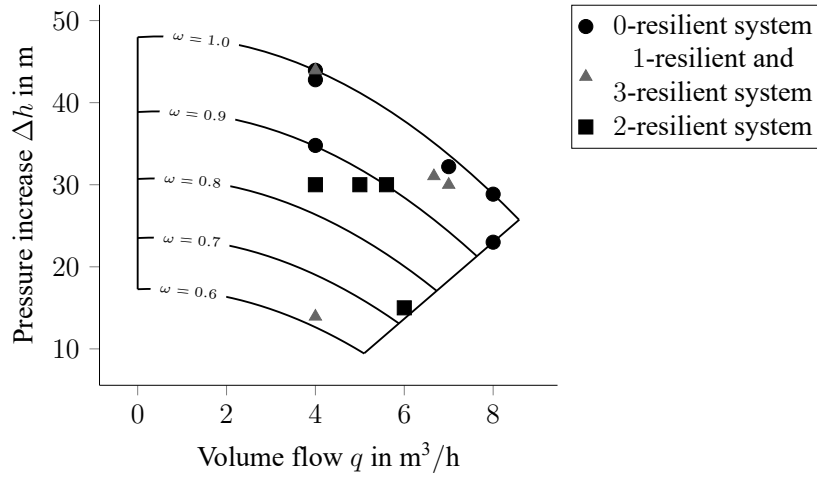


Fig. 3: Operating points of pump Type 3 for each level of k -resilience.

used. Therefore it is possible to plot all operating points in one diagram. The operating points of the 1-resilient and 3-resilient design are equivalent, since both use the same pumps in the case of no failure. The more resilient system designs ($K \geq 1$) are built with higher performance reserves in comparison to the 0-resilient system, where most pumps are used at the upper border of the characteristic diagram.

The maximum pressure increase of the considered pump Type 3 is around 50 meters, cf. Fig. 3. This means, that it is not possible to use multiple parallel pumps of this type to supply all floors, if this group is placed in the ground level of the 100 meter tall building. However, in typical system designs it is common to install only one pump or a smaller group of parallel pumps in the basement. For this consideration, another pump type had to be chosen. If we compare our solution to a booster station designed with the common central approach, our decentralized system has a significantly lower energy demand of up to 30% for the considered load scenario.

To further compare the solutions, we computed for each solution the maximal total volume flow the system can handle after a given number of worst-case failures. In Fig. 4 the ratio of the computed total maximal flow divided by the design point demand D is plotted. For no pump failures, we observe that the overall provided system power is oversized for resilient solutions. Obviously, the maximal demand is below the minimal functionality, if the number of disabled pumps is greater than the guaranteed K . The values of the solutions with buffering capacity of 1 and 2 are slightly above the minimal functionality after one and two worst-case failures, respectively. This stems from the fact, that there are only finitely many water network solutions. Interestingly, the $K = 2$ solution is able to handle more total flow than the solution with capacity 3 for no and one disabled pump.

One simplification used in Model (11) is given by the evenly distributed demand, i.e., the total demand of the building is distributed as $(d_1, \dots, d_N) = (\frac{1}{N}, \dots, \frac{1}{N})$, where $d_v D$ is the demand of pressure zone v . To investigate a deviation from this design point, we parameterize one class of distributions in a degree $\lambda \in [-1, 1]$ for the $N = 7$ pressure zones by

$$(d_1, d_2, d_3, d_4, d_5, d_6, d_7) = \begin{cases} (\frac{1-\lambda}{7}, \frac{1}{7}, \frac{1-\lambda}{7}, \frac{1}{7}, \frac{1-\lambda}{7}, \frac{1}{7}, \frac{1}{7} + 3\lambda), & \text{if } \lambda \geq 0, \\ (\frac{1}{7}, \frac{1+\lambda}{7}, \frac{1}{7}, \frac{1+\lambda}{7}, \frac{1}{7}, \frac{1+\lambda}{7}, \frac{1}{7} - 3\lambda) & \text{else.} \end{cases}$$

For degree $\lambda = 0$, we obtain the design point. For $\lambda > 0$, the demand of every other node starting in node 1 is shifted linearly into the highest node. Whereas, for $\lambda < 0$ the demand of every other node starting in node 2 is shifted into the highest node. We sampled λ and computed for each solution topology the maximal total flow for the flow distribution parameterized by λ . Moreover, we calculated these values for up to three worst-case failures. The different behavior of the optimal topologies is presented in Fig. 5. Note, that the depicted functions are not continuous and only one class of distributions is characterized. The values for $\lambda = 0$ correspond to the values depicted in Fig. 4. The plots are

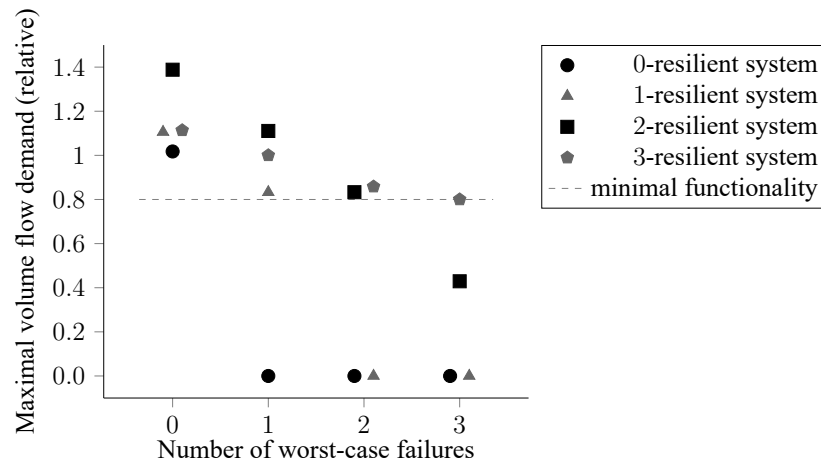


Fig. 4: Maximal demand after worst-case failures for different buffering capacities.

not symmetric, since the pumps in the solutions are not evenly distributed into even and odd pressure zones.

One can see, that the solutions are quite sensitive to the distribution of flow. Further, the maximal possible total demand is always given in the design point for $\lambda = 0$. Compared to the optimal solution, the resilient topologies are less affected by deviations of the demand distribution. Moreover, the topologies optimized for pump failures lie above the minimum function for a wider range of λ . Thus, they are more stable and more resilient than the $K = 0$ solution. Some solutions exhibit plateaus around $\lambda = 0$, which can be explained as follows. For fixed λ , a zone is noted critical, if the pressure condition in this zone is violated by slightly increasing the total demand. For λ on the mentioned plateaus, the critical zones are only supplied by pumps on arc $(0, 1)$. This pipe always transports the same portion of flow regardless of λ , since the changing of demand in the nodes starts in zone 1. Thus, a change in λ does not change the flow in the pumps on this arc. This can be illustrated for the $K = 3$ solution without failures. For $\lambda \in [-0.78, 0.615]$ the critical zone is 2. For other λ , the critical zone changes and is also connected to pumps whose flow is affected by λ . Thus, sudden changes in the functions are based on a change in the critical zone and/or the change of the worst-case failure.

Summary

We presented a model to quantify resilience for water network systems and showed a method based on mathematical optimization to design energy efficient water supply systems which tolerate pump failures. For an exemplary application, we showed that the interconnection of the system components allows to obtain non-trivial solution topologies. The optimized solutions are furthermore more robust with respect to changes from the design point. Overall we achieved an increase of the system's resilience, while the costs of the system were optimized.

The fact that the resilient system with only one branch has similar value than the optimal solution leads to future work, which will focus on the dependency of the solutions on the ratio of the investment versus energy costs in the objective function. We also want to improve the model's accuracy by including nonlinear friction constraints and additional pressure losses for single components like junctions. More different pump types and their possible interconnection should also be considered in the planning phase to validate our results, which often only use one type. A further consideration of resilience with more measures besides the buffering capacity is also planned. Next to the aforementioned water supply system, we want to use the developed methods to investigate the resilience capabilities of further technical systems.

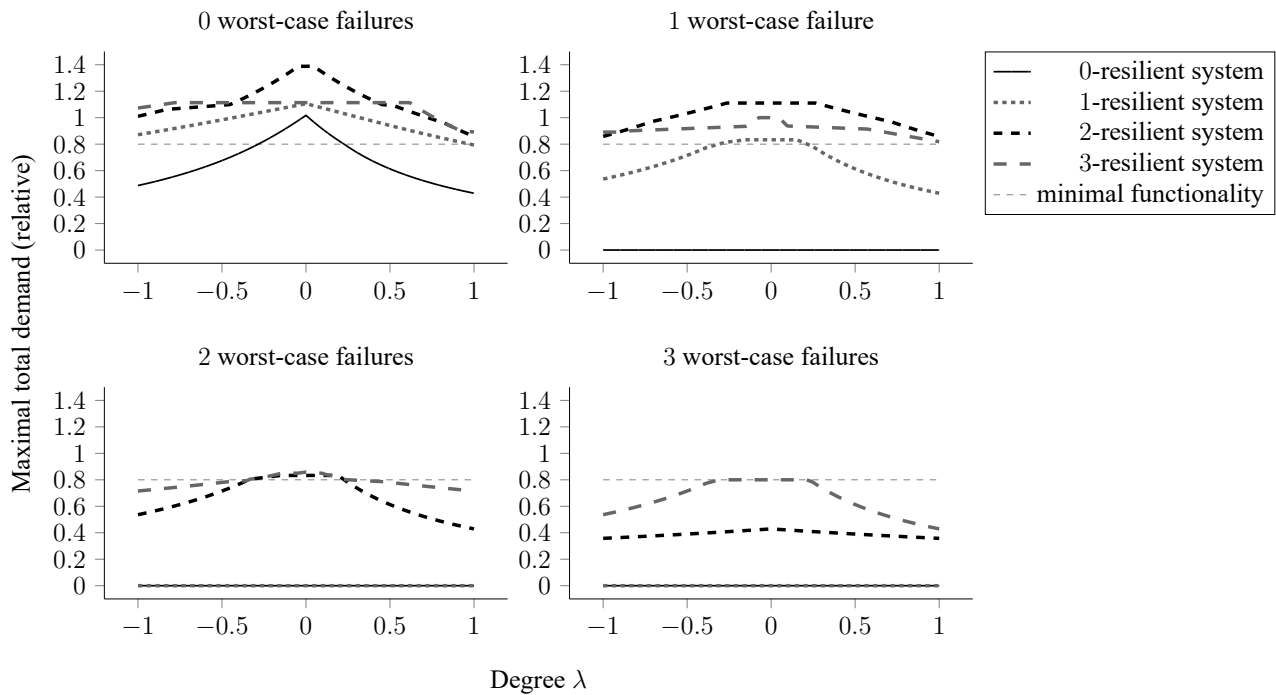


Fig. 5: Maximal demand after worst-case failures for a changing degree of demand distribution to the highest node.

Acknowledgment

The authors thank the German Research Foundation, DFG, for funding this research within the Collaborative Research Center SFB 805 "Control of Uncertainties in Load-Carrying Structures in Mechanical Engineering".

References

- [1] P. Leise, L. C. Altherr, and P. F. Pelz, "Energy-efficient design of a water supply system for skyscrapers by mixed-integer nonlinear programming," in *Operations Research Proceedings 2017*, pp. 475–481, Springer, 2018.
- [2] A. Gleixner, H. Held, W. Huang, and S. Vigerske, "Towards globally optimal operation of water supply networks," *Numerical Algebra, Control and Optimization*, vol. 2, no. 4, pp. 695–711, 2012.
- [3] C. D'Ambrosio, A. Lodi, S. Wiese, and C. Bragalli, "Mathematical programming techniques in water network optimization," *European Journal of Operational Research*, vol. 243, no. 3, pp. 774–788, 2015.
- [4] A. Morsi, B. Geißler, and A. Martin, "Mixed integer optimization of water supply networks," in *Mathematical Optimization of Water Networks* (A. Martin, K. Klamroth, J. Lang, G. Leugering, A. Morsi, M. Oberlack, M. Ostrowski, and R. Rosen, eds.), pp. 35–54, Springer, 2012.
- [5] J. B. Weber and U. Lorenz, "Optimizing booster stations," in *Proceedings of the Genetic and Evolutionary Computation Conference Companion*, pp. 1303–1310, ACM, 2017.
- [6] E. Todini, "Looped water distribution networks design using a resilience index based heuristic approach," *Urban Water*, vol. 2, no. 2, pp. 115–122, 2000.

-
- [7] R. Baños, J. Reça, J. Martínez, C. Gil, and A. L. Márquez, “Resilience indexes for water distribution network design: A performance analysis under demand uncertainty,” *Water Resources Management*, vol. 25, no. 10, pp. 2351–2366, 2011.
- [8] Z. Zhang, X. Feng, and F. Qian, “Studies on resilience of water networks,” *Chemical Engineering Journal*, vol. 147, no. 2-3, pp. 117–121, 2009.
- [9] E. Hollnagel, D. D. Woods, and N. Leveson, *Resilience engineering: Concepts and precepts*. Aldershot, UK: Ashgate, 2006.
- [10] B. Ulanicki, J. Kahler, and B. Coulbeck, “Modeling the efficiency and power characteristics of a pump group,” *Journal of Water Resources Planning and Management*, vol. 134, no. 1, pp. 88–93, 2008.
- [11] T. Groß, P. Pöttgen, and P. F. Pelz, “Analytical approach for the optimal operation of pumps in booster systems,” *Journal of Water Resources Planning and Management*, vol. 143, no. 8, p. 04017029, 2017.
- [12] “DIN 1988-300: Codes of practice for drinking water installations – Part 300: Pipe sizing; DVGW code of practice,” 2012.
- [13] A. Gleixner, L. Eifler, T. Gally, G. Gamrath, P. Gemander, R. L. Gottwald, G. Hendel, C. Hojny, T. Koch, M. Miltenberger, B. Müller, M. E. Pfetsch, C. Puchert, D. Rehfeldt, F. Schlösser, F. Serrano, Y. Shinano, J. M. Viernickel, S. Vigerske, D. Weninger, J. T. Witt, and J. Witzig, “The SCIP Optimization Suite 5.0,” Tech. Rep. 17-61, ZIB, Takustr.7, 14195 Berlin, 2017.